

Rapid Virtual Prototyping of Electric Vehicles Using DQ Behavioral Model of a Brushless DC Motor

Ian Cooper, Peter Wilson, *Senior Member, IEEE*, and Andrew D. Brown *Senior Member, IEEE*,

Abstract—This paper presents a system level for the effective and rapid design and evaluation of a complete electric vehicle system. Several critical components are examined including the mechanical model of the vehicle, the electric motor (with its associated power electronic components) and the energy storage system. A Brushless DC (BLDC) motor Saber model that integrates the DQ axis transformations within the electro-mechanical motor model is developed that facilitates fast and accurate characterization of the behaviour of the vehicle with a realistic drive cycle and aerodynamic model. The simulated results presented show that the novel Saber model can be a viable solution for behavioural high speed analysis of an electric vehicle drive train. The impact on total vehicle simulation times is significant, with a major reduction in simulation times allowing multiple scenarios and optimization of both the system and electronic control to be rapidly undertaken.

Index Terms—Electric Vehicles, Mixed Domain Simulation, Behavioural Modelling

I. INTRODUCTION

PETROL and diesel engines are currently the default choice for traction in transport systems in automotive, rail and static applications; including remote power generation. In the automotive industry this is primarily due to a combination of factors such as fuel energy density, availability and existing supply infrastructure. Petrol (Gasoline) has an extremely high energy density of 13kWh/kg and is therefore able to provide ranges far in excess of the current electric vehicles on the market, due to the relatively low energy density of current battery technology. For example, even modern lithium ion batteries have a considerably lower energy density of approximately 100Wh/kg [1], [2]. In addition, despite much effort being expended in aerodynamic improvements and vehicle weight reduction to improve efficiency, fossil fuel based vehicles are still incredibly inefficient with a large amount of energy being wasted through heat loss and mechanical friction within the engine [3].

In spite of the apparent drawbacks of moving to electric drives for automotive power, there is clear legislative motivation for the adoption of electric vehicles to reduce the carbon footprint of transportation and, there has been a global drive towards electric vehicles as a result [4]. Recently, commercially available hybrid technology has provided a stepping stone to purely electric vehicles [5]. However, while this has been a progressive step and a viable solution for a practical day-to-day car, there are clear cost disadvantages in having multiple power

plants (petrol + electric), and a complex control mechanism to manage both [6].

The long term automotive trend is clearly towards purely electric vehicles, with the prospect of much cheaper running costs and significantly simpler manufacturing and maintenance due to the reduction in complex moving parts [7], [8].

The key elements in a purely electric drive-train, as illustrated by Fig 1, are the motor, power electronics and energy storage. There is already a plethora of research into different power sources, see [9]–[12], including batteries and alternative fuel options such as hydrogen. Quickly changeable battery packs have also been researched, as in [13], which would allow the vehicle to be operated by the driver in a similar fashion to filling up with petrol, resulting in effective increased range. While this is a useful step forward, the actual form of electricity storage is beyond the scope of this paper, however it does strengthen the argument that Electric Vehicles are becoming increasingly viable and will have a larger share of the automotive market as a result.

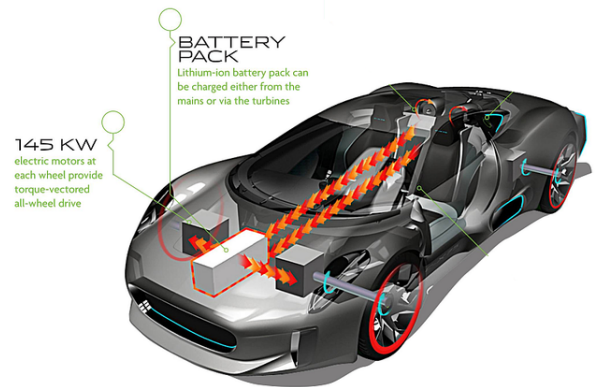


Fig. 1: Jaguar C-X75 Electric Vehicle Concept, modified from [14]

Obviously, the most important moving part in an Electric Vehicle (EV) drive-train is the electric motor itself, and it is vital that the motor is carefully selected in order to utilise the stored energy as efficiently as possible. Electric motors, powered by on board batteries, have the potential to revolutionise vehicle drive systems by increasing efficiency and even delivering a higher power to weight ratio over their internal combustion engine equivalents. The reduction in complexity, particularly of moving parts, is also a huge advantage, so the benefits to the motorist are potentially wide ranging.

There are numerous potential options for electric motors including DC permanent magnet (DCPM), AC Induc-

P.R. Wilson and A.D. Brown are with the School of Electronics and Computer Science, University of Southampton, Southampton, SO17 1BJ (email:prw@ecs.soton.ac.uk) and I. Cooper is with Jaguar Land Rover, UK

tion, Switched Reluctance [15] and DC Brushless. Brushed (DCPM) and Brushless DC motors (BLDC) are both considered to be viable options to use to replace an internal combustion engine, each has advantages and disadvantages within the context of an electric vehicle [16], although most forms of electric motor have been attempted in some form of electric vehicle conversion in recent years.

BLDC motors have several key advantages over brushed DC motors. BLDC motors are not mechanically commutated by brushes and a commutator; this offers some attractive characteristics for electric vehicle use. Higher efficiency and reliability, higher power density, reduced noise and a longer lifespan due to the design having less components that wear. Recent research indicates the viability and flexibility of DC Brushless Motors for this application [17], [18].

DC PM motors are still a viable option, however, an obvious important disadvantage to consider is that the design uses brushes. Degradation of performance over time, and the reduced time between maintenance are important aspects to consider when designing a vehicle that is to run for a long time. Therefore, this paper will focus on BLDC motors, as a suitable target technology for electric vehicle power trains.

In the automotive industry, there are several options for predicting electric vehicle power train performance, including simulators such as Matlab, Saber and SPICE. In practice, Matlab and other system level simulators are focussed on a macro level simulation of vehicle performance and drive cycles; the SPICE type simulators are used to carry out detailed level simulations of electronic components [19], [20]. Other options are also available, including the use of mixed-technology simulators such as Saber, a standard for many automotive companies including GM and Ford, and these have the advantage that it is possible to analyse all aspects of the EV power train from system down to device level [21]. An important aspect to consider is that using a mixed-technology level means that a true energy conserved model is analysed which aids in the understanding of the efficiency of the entire system.

This mixed domain context it is extremely valuable in modelling and simulation of the electric vehicle power train from source to wheel [22], [23]. It is therefore important to be able to model not only the control and system aspects of the power train, but also the electrical and mechanical behaviour accurately. Due to the industry requirement to simulate vehicle dynamics under varying conditions for long periods it is important that simulations be run quickly. Simulation of motor performance for changing external conditions such as high acceleration and high speed demands is essential. This can be a particular issue when detailed cycle by cycle modelling of power electronics are required, however for system level design and optimization rapid simulation is essential.

Conventional methods of modelling motor drive systems have used equivalent models based on the well known Park and Clarke transforms, which combine the DQ axis control model with three phase motor models, however this still requires a full multi-phase model of the motor and the associated power electronics to be simulated. While this approach is relatively accurate, it has a significant impact on simulation

time in comparison to a high level system model. A potentially interesting alternative approach is to implement an integrated motor/driver model; alleviating the need for many complex transforms by implementing the resulting DQ axis model directly. [24].

Given these requirements, the purpose of this paper is therefore to design and implement a fully integrated model for fast system simulation whilst being able to integrate mechanical, control and electronic aspects. The proposed DQ BLDC motor model implemented in this paper is compared against a conventional 3 phase model. Simulation results are given to illustrate the performance of the proposed model from a system designer's perspective.

This paper will therefore introduce the key concepts in Brushless DC Motor operation and control in Section II, Section III will develop the new BLDC model including a comparison with previous models, Section IV will show how this can be used for rapid evaluation of electric vehicle system models and finally Section V will provide a conclusion.

II. ELECTRIC VEHICLE SYSTEM MODEL

In order to establish the basic vehicle performance at the system level, a behavioral model of the motor, power electronics and mechanical system is required. The initial model created in Saber to establish the key elements of the vehicle behavior is shown in Fig 2. The model has an initial assumption of an ideal energy store (in other words, although in reality the battery voltage would "droop" under load, and the power electronics would need to compensate for this, at this initial stage the model assumes a relatively ideal starting point. The power electronics is modelled as an ideal power system, with no switching, but with time constants and loop behaviour. The outer control loop is based on speed control, where the speed demand will be one of the European Union standard cycles (for example ECE15 [25] which is the light urban test cycle).

The motor is represented by an ideal system level model of a motor using ideal motor equations, and is therefore not intended at this stage to accurately reflect the physical behaviour or detailed control requirements of the individual motor. The mechanical model includes the mass of the vehicle, aerodynamic drag and rolling resistance, with calculations of the vehicle speed, acceleration and distance. The resulting simulation of this model shows how the system level model can be used to predict the speed (against the demanded ECE profile), distance travelled (in meters) and power required at each stage.

This initial model is therefore useful in establishing the power budget of the vehicle, however it does not really offer a particular step forward in itself over previous system level models, in particular in improving the model of the motor without resorting to excessive detail. The next section of this paper will therefore introduce the design issues in using brushless DC motors and the challenge for accurately modeling them quickly and efficiently.

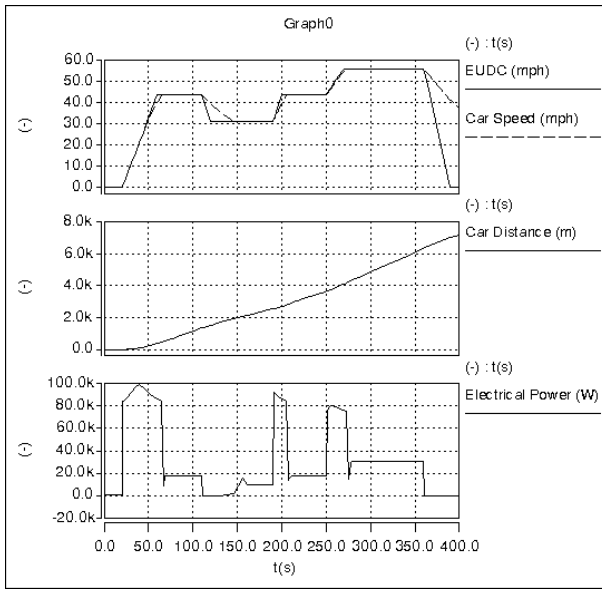


Fig. 3: Electric Vehicle Simulation Results



Fig. 4: BLDC Motor

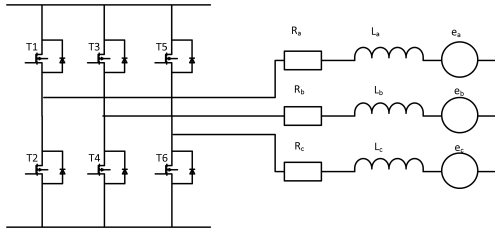


Fig. 5: BLDC Equivalent circuit

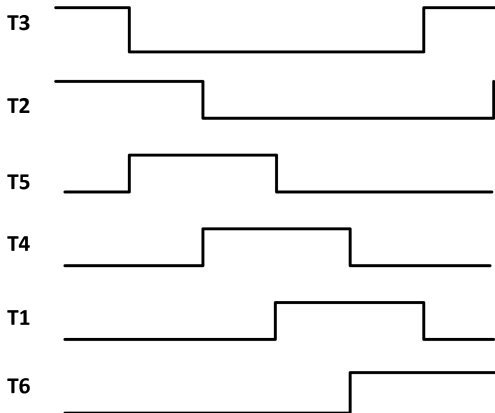


Fig. 6: BLDC Commutation Sequence

III. BRUSHLESS DC MOTOR OPERATION AND CONTROL

Brushless Direct Current (BLDC) Motors, as already discussed, are an excellent choice for use in an electric vehicle

drive system due to their relatively high efficiency and low maintenance. Fig 4 shows the equivalent circuit of a typical BLDC motor. The rotational speed of a BLDC motor is directly proportional to the applied voltage across the motor coils. In a DC motor the brushes and commutator act like a rotary switch, selecting which of the coils to power to achieve rotation through mechanical commutation. Unlike DC motors, BLDC motors require external electronics to control motor commutation, adding an extra level of complexity to the system [26].

Driver circuits are required by BLDC motors to provide the correct commutation sequence to make the motor turn [27]. Fig 5 shows the driver circuit for a typical BLDC motor. In order to operate the motor and produce rotational torque at the output shaft each coil must be electrically excited synchronously with the current rotor position. The equivalent circuit, shown in Fig 5, is connected to a three-phase full-bridge circuit. This circuit is used to provide electrical excitation of the motor coils in a given direction and acts as the DC link between the motor and the controller. Each transistor is driven independently by an external controller; the commutation sequence shown in Fig 6 is performed to allow the motor to turn. To vary the rotational speed of the motor the transistors in each pair can be pulse width modulated, varying the average DC voltage across the motor winding [28]. The motor will be running at full speed if the transistors are driven for the full time period of the 120 electrical degrees. Since only 2 phases of the 3 are excited at any time trapezoidal back-EMF is generated in the unexcited winding. This is an effect of the generating properties of electric motors. This back-EMF, is aligned with the phase current and this can be utilised in sensorless control.

The electronic control of BLDC motors requires rotor position feedback in order to operate. This is approached either with sensors, or without, known as 'sensor-less' feedback. Both methods allow the control circuit to synchronise with the motor, and are occasionally used to provide an external RPM (revolutions per minute) value. Typically Hall sensors are used to detect where in the commutation cycle the rotor is by detecting the different magnetic fields as the magnetic poles of the commutator pass. However, Hall sensors have a maximum operating temperature and increase the cost and size of the motor. The sensors are also fragile and, mounting inaccuracies in manufacture can affect switching accuracy. [27]–[30].

Sensor-less control techniques for BLDC motors have been a highly researched area in recent years and a number of approaches have been proposed [30], [31]. Sensorless operation involves detection of the terminal voltage of the motor poles in conjunction with the switching sequence; using the generated trapezoidal back-EMF to synchronize and control the motor [28]. Multiple methods exist for sensorless motor control. Algebraic, equation based control techniques exist, which utilise calculated flux linkages or model predictions to calculate rotor position and speed [31]. Through monitoring of the back-EMF in the silent phase, the zero crossing point can be detected. The measured commutation points are then phase shifted by 30°, requiring a speed-dependant time delay citeControlTechniques:Paper. The BLDC motor can then be synchronized without the need for sensors [28]. Several tech-

niques utilise back-EMF voltage sensing to synchronise the motor. These include but are not limited to: Terminal Voltage Sensing, Third Harmonic back-EMF voltage sensing and free-wheel diode conduction [29], [31].

Terminal voltage sensing provides a simple system in comparison to others, with minimal extra hardware component requirements. This simplicity at a hardware level means this technique is widely used within industry [30]. However, since the 30° speed dependant phase delay can cause large differences in actual rotor position. This can limit the maximum torque from the motor due to incorrect commutation sequence alignment. A study in to maximum torque generation using terminal voltage sensing is presented here [27]. Terminal voltage sensing is ideal for implementation on a micro controller as in [29], [30]. Built in A to D converters as well as PWM outputs commonly built in to modern micro controllers, make them a low cost solution to BLDC control.

A fuzzy logic control (FLC) implementation using a micro controller is [28]. This removes some computation required at run time by the micro controller, calculating values at programming time and placing them into a look up table (LUT). This is similar in concept to that of the simulated novel BLDC motor model discussed in this paper. Switching instants can also be determined using the third harmonic of the back-EMF. Measuring the voltage between the virtual neutral point and the negative voltage rail allows the third harmonic flux linkage through integration of voltage. [30]. This technique is not as susceptible to phase delay of conduction sequence as terminal voltage sensing [31].

While it is beyond the scope of this paper to descend into the detail of designing a brushless DC motor controller, it is clear that while system level simulators such as Matlab are ideally suited to the high level equations of a system level description, the detail required for a switch level simulation would lead to prohibitively long simulation times for any kind of cycle testing as described in the previous section of this paper, with test times measured in minutes or even hours. This is driving towards the use of a "hybrid" level model that can encompass the basic system level behaviour and yet maintain enough detail to enable optimization and design of key motor and power electronic parameters. This will be developed in the next section of this paper.

IV. DQ AXIS BLDC BEHAVIORAL SABER MODEL

There has been a significant effort into the development of models for Brushless DC motor models, with the obvious use of the DQ transformation to simplify the control and drive aspects of the system model. Recent work has also taken the approach of modelling the DQ axis behaviour in order to accurately model the detailed harmonics in the system [32], however this is not the main requirement of the model in this case. The classic approach used to model and implement control in three phase BLDC systems is to transform the demand and feedback current and voltages from the 3 phase domain into an equivalent DQ axis. This is extremely useful for control algorithms, and also has the advantage from a modelling perspective of simplifying the system model into the

same DQ axis. The basic approach of just the transforms and BLDC model is shown in 7. The detailed magnetic behaviour of the windings has not been included in this initial model, however the non-linear magnetics can be modelled using standard approaches such as the Jiles-Atherton model [33], [34], [35], with the ability to predict the effects of hysteresis on distortion [36] or losses [37]. The other important aspect of modelling behaviour in electric vehicles would be the effects of temperature on the magnetic material performance which can have a profound effect on the motor winding inductance [38].

The transformation of the ABC currents into the DQ axis is transformed using the well known dq0 transformation using the relation defined in Equation 1 with the transformation matrix defined in 2.

$$I_{dq0} = T I_{abc} = \sqrt{\frac{2}{3}} \begin{bmatrix} DQ0 \\ \end{bmatrix} \begin{bmatrix} I_a \\ I_b \\ I_c \end{bmatrix} \quad (1)$$

$$\begin{bmatrix} DQ0 \\ \end{bmatrix} = \begin{bmatrix} \cos(\phi) & \cos(\phi - \frac{2\pi}{3}) & \cos(\phi + \frac{2\pi}{3}) \\ -\sin(\phi) & -\sin(\phi - \frac{2\pi}{3}) & -\sin(\phi + \frac{2\pi}{3}) \\ \frac{\sqrt{2}}{2} & \frac{\sqrt{2}}{2} & \frac{\sqrt{2}}{2} \end{bmatrix} \quad (2)$$

Conversely, the transformation from the DQ axis into the dq0 reference frame requires the opposite transformation as shown in Equation 3 and the inverse matrix in 4.

$$I_{abc} = T^{-1} I_{dq0} = \sqrt{\frac{2}{3}} \begin{bmatrix} DQ0^{-1} \\ \end{bmatrix} \begin{bmatrix} I_d \\ I_q \\ I_o \end{bmatrix} \quad (3)$$

$$\begin{bmatrix} DQ0^{-1} \\ \end{bmatrix} = \begin{bmatrix} \cos(\phi) & -\sin(\phi) & \frac{\sqrt{2}}{2} \\ \cos(\phi - \frac{2\pi}{3}) & -\sin(\phi - \frac{2\pi}{3}) & \frac{\sqrt{2}}{2} \\ \cos(\phi + \frac{2\pi}{3}) & -\sin(\phi + \frac{2\pi}{3}) & \frac{\sqrt{2}}{2} \end{bmatrix} \quad (4)$$

Figure 8 shows the Saber schematic used to simulate a standard Sine approach to BLDC control. The sensorless back-EMF feedback is transformed via the dq0 transform, given by the equation below, so that 2 DC quantities can be used in the control feedback [31]. The d and q values are then used in PI type controllers which allow the motor to maintain constant torque or speed. However, these calculated values must then have the reverse dq0 transform, given by the equation below, applied in order to produce the ABC sinusoid values required by the BLDC motor model. This is the conventional approach to BLDC motor modelling [23].

Figure 8 also shows the dq transform blocks used to translate from the DQ0 axis models to the three phase voltages and currents in a conventional model. These transforms are calculated for every simulation step. Variable time step algorithms, such as those found in Matlab, SPICE or Saber increase the frequency of simulation samples during areas of high interest such as accelerations and decelerations, and in particular if the frequency of the drive system increases. This means that simulations of electric vehicle drive cycles take extra computing time to complete, slowing down the testing

process [32]. To facilitate a solution, and reduce the time taken to simulate complex drive cycles for electric vehicles a novel BLDC motor model is presented in this paper. The model, like the sine model simulated above, takes in a speed demand, however, the dq motor model uses the DC d and q values as inputs, instead of ABC sinusoids. This negates the necessity to have transformations from and to a three phase model, reducing the time taken to simulate the given stimulus. Although both models are behavioural, not monitoring the switching of transistors as in [33], they provide a significantly faster simulation. Figure 9 shows the new DQ motor model based system. The result is that by not requiring to simulate the the actual sinusoidal wave shapes, the model becomes speed and frequency independent and the simulation times are much faster for equivalent accuracy. The approach is to implement the brushless motor equations directly in the DQ axis as shown in Equations 5, 6 and 7.

$$V_q = R_s I_q + L_q \frac{dI_q}{dt} + \omega_e L_d I_d + \omega_e k_t \quad (5)$$

$$V_d = R_s I_d + L_d \frac{dI_d}{dt} + \omega_e L_q I_q \quad (6)$$

$$T_q = I_q k_t \quad (7)$$

The complete listing of the resulting model is given in Appendix A.

V. COMPLETE ELECTRIC VEHICLE SIMULATION MODEL

Most practical testing of electric vehicle performance through simulation requires the simulation to provide stimulus similar to the conditions that may be found in a real world environment. The simulation aids designers with choice of motor since accelerations and high speeds are simulated to find out if the motor and its gearing can provide the torque as well as wheel RPMs required. In order to provide a useful reference vehicle for study, a Toyota MR2 was modified to an electric drive as shown in 10.



Fig. 10: Fully Electric MR2

Typically a driving cycle is used to assess the emission level of a car engine. The cycle is made up from data points in time giving the speed of the vehicle; accelerations, decelerations

and frequent stops are included to provide a unified test to assess vehicle performance [39]. Testing using drive cycle as a stimulus is a more accurate test than testing constant vehicle speed simulation, as this condition would be impossible to achieve on real roads. The European driving cycle, ECE-15, can be used to get a good idea of an electric vehicles' performance and range [39].

In simulation the speed demand fed in to the motor controller is provided by the drive cycle, testing the acceleration, deceleration and fixed speed of the vehicle. The system model is then used to connect the physical properties of the moving vehicle to the motor in order to properly simulate the motor powering a car such as the University of Southampton Electric MR2, shown in Fig 10. When a step change speed demand was applied to the vehicle, the resulting acceleration of the vehicle was observed in the model and the simulation tie observed. As can be seen in 11, the vehicle reaches the required speed correctly, however as can be seen in I, the simulation time is a fraction of that for the sinusoidal model.

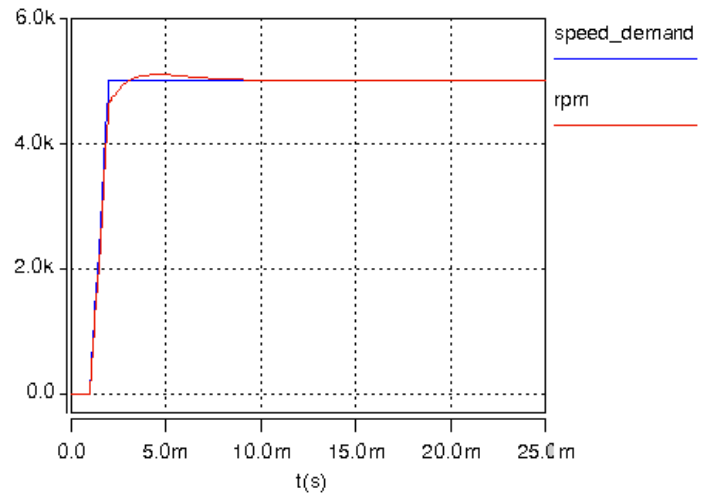


Fig. 11: DQ motor test

Model	Simulation Time (s)
New DQ Motor	5.54
Conventional three phase Brushless Motor Model	198.0

TABLE I: Results

VI. CONCLUSIONS

A novel BLDC motor model has been simulated successfully in this paper using mixed domain simulation in Saber. The results show that the behavioural simulation conducted with a variable speed demand over a long period significantly favour the new model over a more conventional sine model in terms of calculation time.

The model in this paper, which eliminates the necessity for complex transformations at simulation run time, requires less computation time for the same external conditions; an ideal characteristic for electric vehicle simulation.

In comparison to other models the new model allows for longer simulations to be performed in shorter times, enabling

a high level of simulation to be performed and allowing informed considerations of motor choice during the electric vehicle design phase.

VII. APPENDIX A: SABER MODEL LISTING

```

template dqmotor q d t=rs,ld,lq,kt,p,eff
electrical q,d
rotational_vel t
number rs=10m
number ld=100u
number lq=100u
number kt=0.1
number p=1
number eff=0.95
{
electrical n
val v vq
val v vd
var i iq
var i id
var i diddt
var i diqdt
val tq_nm tq
val f phiq
val f phid
val w_radps w
val w_radps we
val p_mech_power
val p_elec_power
val nu efficiency

number imax = 1000

values {
    vq=v(q)-v(n)
    vd=v(d)-v(n)

    # calculate rotor speed:
    w=w_radps(t)

    phid = id*ld
    phiq = iq*lq

    tq = (3/2)*(kt*iq*eff*(1-abs(iq)/imax))
    efficiency = eff*(1-abs(iq)/imax)

    we = w*p

    mech_power = tq * w
    elec_power = (3/2) * (vq*iq + vd*id)
}

equations{
    i(q->n)+=iq*3/2
    i(d->n)+=id*3/2
    tq_Nm(t) += tq
    iq: vq=rs*iq + lq*diqdt + we*ld*id + we*kt

```

```

iq: tq = iq*kt*efficiency
id: vd=rs*id + ld*diddt - we*lq*iq
diqdt: diqdt=d_by_dt(iq)
diddt: diddt=d_by_dt(id)
}

```

```

short.1 n 0
}

```

REFERENCES

- [1] M. I. Research, "High impedance battery research," 2005.
- [2] K. Kariatsumari, "Toshiba boosts energy density of li-ion battery by 502009.
- [3] J. Larminie and J. Lowry, *Electric Vehicle Technology Explained*. New York: Wiley, 2003.
- [4] U. Nations, "Kyoto protocol," 2008.
- [5] V. Sreedhar, "Plug-In Hybrid Electric Vehicles with Full Performance," *Electric and Hybrid Vehicles Conference*, pp. 1–2, 2006.
- [6] S. Stockar, V. Marano, M. Canova, G. Rizzoni, and L. Guzzella, "Energy-Optimal Control of Plug-in Hybrid Electric Vehicles for Real-World Driving Cycles," *IEEE Transactions on Vehicular Technology*, vol. 60, pp. 2949–2962, 2011.
- [7] D. Willman, "Positive trends sparking the second generation of electric vehicles," 2012.
- [8] P. Convington, "Stronger u.s. sales of hybrids and plug-in electrics in march," 2012.
- [9] H. J. Schwartz, "The computer simulation of automobile use patterns for defining battery requirements for electric cars ." NASA Technical Memorandum, NASA Tm X-71900, 2006.
- [10] D. L. Harbaugh, "Electric-vehicle commuter car battery requirements ," *WESCON, USA*, pp. 28–32, 1994.
- [11] M. Winter, "Lithium ion batteries as key component for energy storage in automotive and stationary applications ," *INTELEC, Germany*, pp. 1–3, 2011.
- [12] C. Goia, "Supercapacitors used as an energy source to drive the short urban electric vehicles ," *ICPE, Romania*, pp. 1–6, 2011.
- [13] L. Tan, "A robotic system design based on electric passenger car battery quick-change ," *Conference on Electornics, Communications and Control, China*, pp. 4116–4118, 2011.
- [14] "Jaguar introduces c-x75 gas micro-turbine extended range electric vehicle concept," 2010.
- [15] J. Kim, K. Ha, and R. Krishnan, "Single-controllable-switch-based switched reluctance motor drive for low cost, variable-speed applications," *Power Electronics, IEEE Transactions on*, vol. 27, pp. 379–387, jan. 2012.
- [16] X. D. Xue, "Selection of Electric Motor Drives for Electric Vehicles ," *AUPEC, Hong Kong*, pp. 1–6, 2008.
- [17] J.-H. Choi, Y.-D. Chun, P.-W. Han, M.-J. Kim, D.-H. Koo, J. Lee, and J.-S. Chun, "Design of High Power Permanent Magnet Motor With Segment Rectangular Copper Wire and Closed Slot Opening on Electric Vehicles," *IEEE Transactions on Magnetics*, vol. 46, no. 6, pp. 2070–2073, 2010.
- [18] P. Kumar and P. Bauer, "Improved Analytical Model of a Permanent-Magnet Brushless DC Motor," *IEEE Transactions on Magnetics*, vol. 44, pp. 2299–2309, 2008.
- [19] K. Butler, M. Ehsani, and P. Kamath, "A Matlab-based modeling and simulation package for electric and hybrid electric vehicle design," *IEEE Transactions on Vehicular Technology*, vol. 48, pp. 1770–1778, 1999.
- [20] A. Fardoun, E. Fuchs, and H. Huang, "Modeling and simulation of an electronically commutated permanent-magnet machine drive system using SPICE," *Industry Applications Society Annual Meeting, CO, USA*, vol. 1, pp. 439–447, 1994.
- [21] C. M. D. W. Gao and A. Emadi, "modeling and simulation of electric and hybrid vehicles"," *Proceedings of the IEEE*, vol. 95, pp. 729–745, 2007,.
- [22] S. Wirasingha, R. Gremban, and A. Emadi, "Source-to-Wheel (STW) Analysis of Plug-in Hybrid Electric Vehicles," *IEEE Transactions on Smart Grid*, vol. 3, pp. 316–331, 2012.
- [23] J.-C. Olivier, G. Wasselynck, D. Ireena, B. Auvity, C. Josset, C. Le-Bozec, and P. Maindru, "Power source to wheel model of a high efficiency fuel cell based vehicle," *VPPC, France*, 2010.
- [24] P. Vas, *Sensorless Vector and Direct Torque Control*. Oxford Science Publications, 1998.

- [25] B. Tabbache, A. Kheloui, and M. Benbouzid, "Design and Control of the Induction Motor Propulsion of an Electric Vehicle," *VPPC, France*, pp. 1–6, 2010.
- [26] J. Titus, "Brushless dc motors: Part 1," 2009.
- [27] C.-G. Kim, J.-H. Lee, H.-W. Kim, and M.-J. Yuon, "Study on maximum torque generation for sensorless controlled brushless DC motor with trapezoidal back EMF," *IEEE Proc. on Electric Power Applications*, vol. 152, pp. 277–291, 2005.
- [28] J.-S. Wen, C.-H. Wang, Y.-D. Chang, and C.-C. Teng, "Intelligent Control of High-Speed Sensorless Brushless DC Motor for Intelligent Automobiles," *Systems, Man and Cybernetics Conference*, pp. 3394–3398, 2008.
- [29] Xionghui and X. YanBo, "The Design of a Brushless DC Motor Back-EMF Control," 2010.
- [30] Y. Kang, S. B. Lee, and J. Yoo, "A Microcontroller Embedded AD Converter based Low Cost Sensorless Technique for Brushless DC Motor Drives," *Industry Applications Conference*, vol. 3, pp. 2176–2181, 2005.
- [31] J. P. Johnson, M. E. Lee, and Y. Güzelgünler, "Review of Sensorless Methods for Brushless DC," *IAS Annual Meeting, TX, USA*, pp. 143–150, 1999.
- [32] K. Tabarraee, J. Iyer, H. Atighechi, and J. Jatskevich, "Dynamic average-value modeling of 120 vsi-commutated brushless dc motors with trapezoidal back emf," *Energy Conversion, IEEE Transactions on*, vol. 27, pp. 296–307, june 2012.
- [33] P. W. J. Ross, "definition and application of magnetic material metrics in modeling and optimization," *IEEE Transactions on Magnetics*, vol. 37, pp. 3774–3780, 2001.
- [34] J. R. A. B. P.R. Wilson, "magnetic material model characterization and optimization software," *IEEE Transactions on Magnetics*, vol. 38, pp. 1049–1052, 2002.
- [35] J. R. A. B. P.R. Wilson, "optimizing the jiles-atherton model of hysteresis using a genetic algorithm," *IEEE Transactions on Magnetics*, vol. 37, pp. 989–993, 2001.
- [36] J. R. A. B. P.R. Wilson, "predicting total harmonic distortion in asymmetric digital subscriber line transformers by simulation," *IEEE Transactions on Magnetics*, vol. 40, pp. 1542–1549, 2004.
- [37] J. R. A. B. P.R. Wilson, "modeling frequency-dependent losses in ferrite cores," *IEEE Transactions on Magnetics*, vol. 40, pp. 1537–1541, 2004.
- [38] J. R. A. B. P.R. Wilson, "simulation of magnetic component models in electric circuits including dynamic thermal effects," *IEEE Transactions on Power Electronics*, vol. 17, pp. 55–65, 2002.
- [39] E.Tzirakis, K. Pisas, F. Zannikos, and S. Stourmas, "Vehicle Emissions and Driving Cycles," *globalNEST*, vol. 8, no. 3, pp. 282–290, 2006.

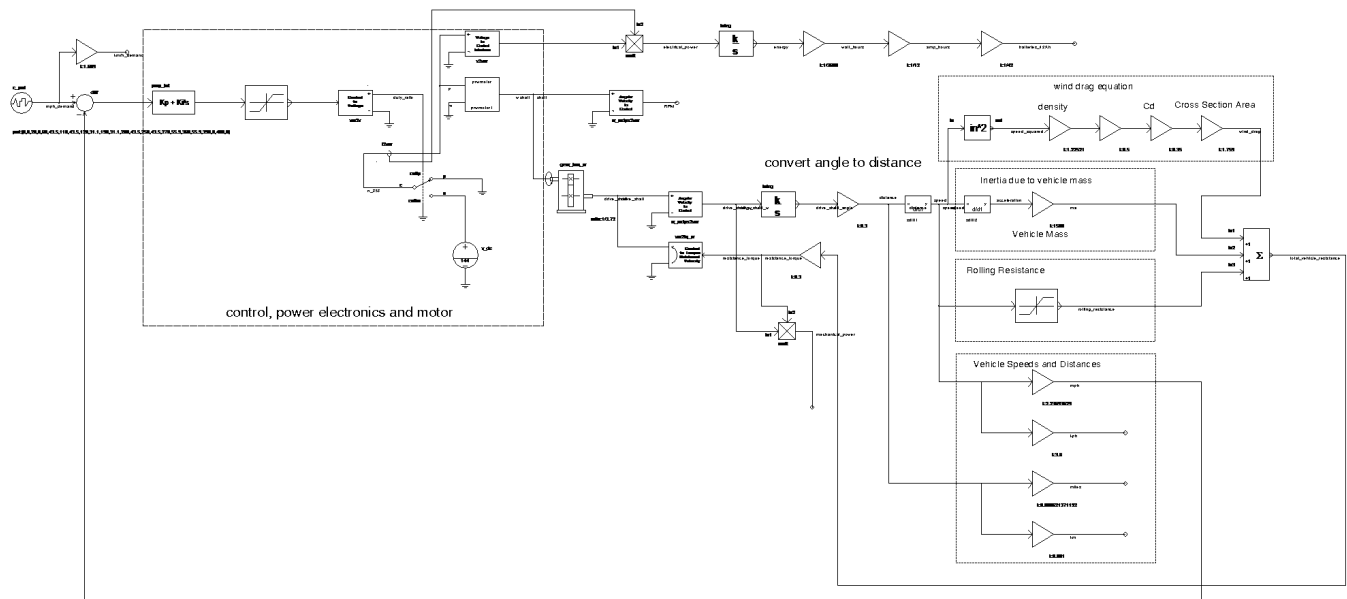


Fig. 2: Electric Vehicle Mixed Domain model

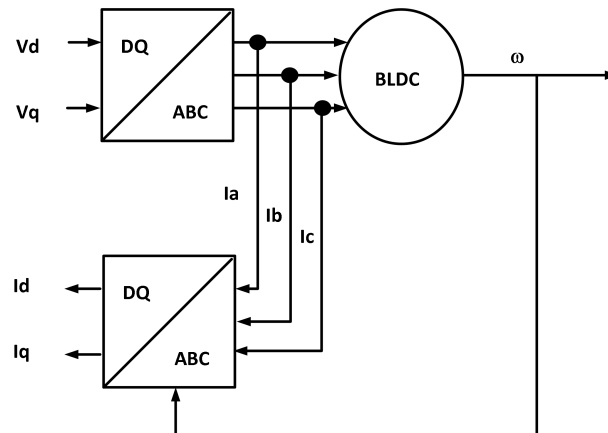


Fig. 7: BLDC and DQ transformation block diagram

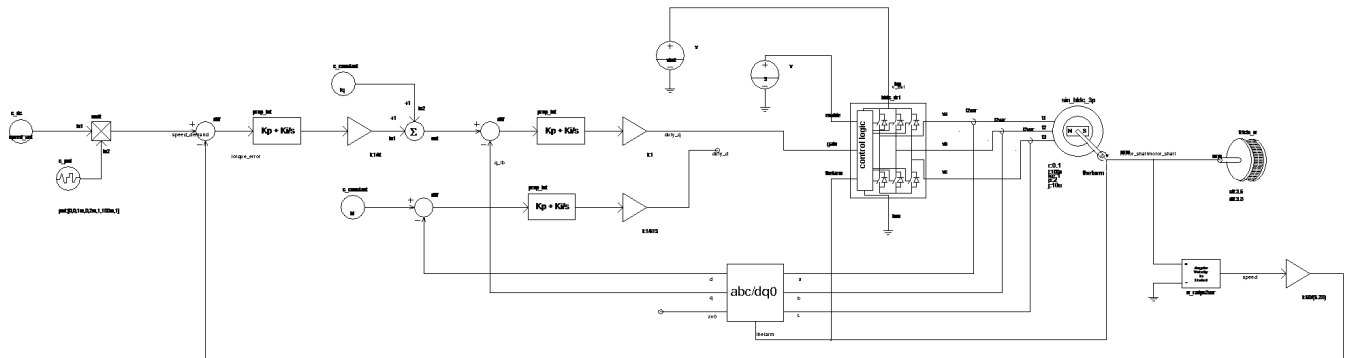


Fig. 8: BLDC Sine cycle test

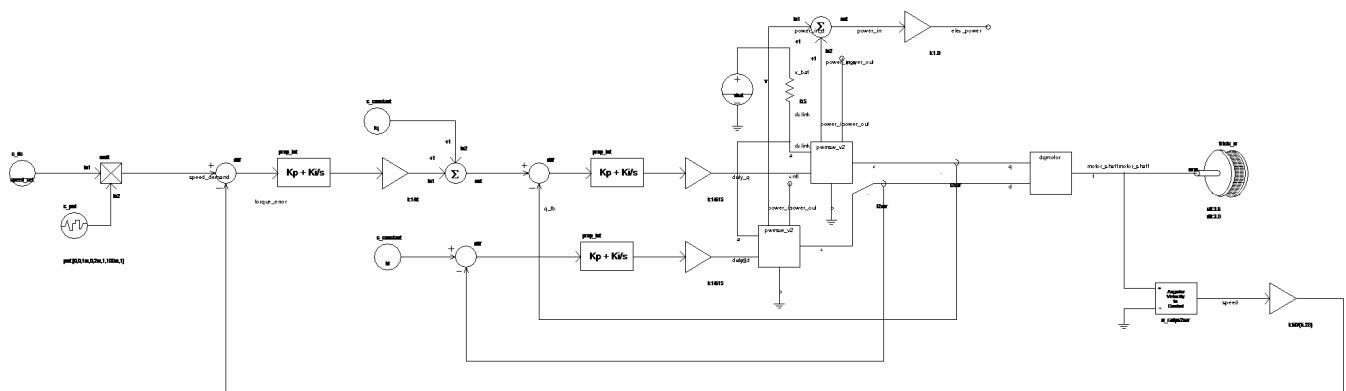


Fig. 9: BLDC novel DQ motor model